

ChemComm

Accepted Manuscript



This is an *Accepted Manuscript*, which has been through the Royal Society of Chemistry peer review process and has been accepted for publication.

Accepted Manuscripts are published online shortly after acceptance, before technical editing, formatting and proof reading. Using this free service, authors can make their results available to the community, in citable form, before we publish the edited article. We will replace this *Accepted Manuscript* with the edited and formatted *Advance Article* as soon as it is available.

You can find more information about *Accepted Manuscripts* in the [Information for Authors](#).

Please note that technical editing may introduce minor changes to the text and/or graphics, which may alter content. The journal's standard [Terms & Conditions](#) and the [Ethical guidelines](#) still apply. In no event shall the Royal Society of Chemistry be held responsible for any errors or omissions in this *Accepted Manuscript* or any consequences arising from the use of any information it contains.

COMMUNICATION

Template-free synthesis of mesoporous polymers

Cite this: DOI: 10.1039/x0xx00000x

Xinxin Sang, Li Peng, Jianling Zhang*, Buxing Han, Zhimin Xue, Chengcheng Liu, and Guanying Yang

Received 00th January 2012,
Accepted 00th January 2012

DOI: 10.1039/x0xx00000x

www.rsc.org/

The mesoporous polyacrylamides (PAMs) with tunable porosities were synthesized in 1-alkyl-3-methylimidazolium tetrafluoroborates ($[C_n\text{mim}][\text{BF}_4]$, $n=4, 6, 8, 10$). The as-synthesized PAM was used as a support for Pd nanoparticles and the Pd/PAM composite shows highly catalytic activity and selectivity for the hydrogenation of *p*-chloronitrobenzene to yield *p*-chloroaniline.

Mesoporous polymers have received an increased interest of research concern because of their potential to coalesce the properties of both mesoporous materials and polymers.¹⁻⁵ Mesoporous polymer materials have exhibited promising potential applications in different areas such as adsorption of large molecules,^{6,7} purification,^{8,9} batteries¹⁰ and energy storage.¹¹ The synthetic strategies of mesoporous polymers include the hard template (e.g. silica or block copolymers) and soft template (e.g. surfactant micelles) techniques.^{1,12,13} The use of templates has obvious disadvantages of high cost, environmental pollution and additional experimental procedures to wipe out the templates. It is desirable to develop the template-free route for the mesoporous polymer formation, but it still remains great challenging.

Ionic liquids (ILs) as a new class of environmental friendly solvents have attracted much attention due to their chemical stability, low vapor pressure, high ionic conductivity and tunable properties (by designing the structures of the cation and the anion).¹⁴⁻¹⁹ Up to now, ILs have been widely used as solvents for chemical reactions,²⁰ material synthesis,^{21,22} polymerization.²³⁻²⁶ However, the use of ILs for synthesizing porous polymers is very limited and the reports were sporadically published.²⁷⁻³⁰ Especially, the fabrication of mesoporous polymers using IL has not been reported until a recent work by utilizing the surfactant micelles in IL as mesopore templates.³⁰

Herein we aim to achieve the template-free synthesis of mesoporous polymers in pure IL. This strategy is based on the fact that ILs are structured and nano-segregated fluids, because the aggregation of alkyl chains in ILs occurs when alkyl chains of

sufficient length are involved, forming nonpolar nanodomains in IL.^{31,32} The route involves no additional template, no volatile organic solvent, and is more environmentally benign. The mesoporous polyacrylamides (PAMs) with tunable porosities were synthesized in 1-alkyl-3-methylimidazolium tetrafluoroborates ($[C_n\text{mim}][\text{BF}_4]$, $n=4, 6, 8, 10$). The as-synthesized PAM was used as a support for Pd nanoparticles and the Pd/PAM composite shows highly catalytic activity and selectivity for the hydrogenation of *p*-chloronitrobenzene (CNB) to obtain *p*-chloroaniline (CAN).

Fig. 1a shows the SEM image of the PAM synthesized in $[C_4\text{mim}][\text{BF}_4]$, from which the particles in size of 50-100 nm can be observed. The TEM images show that the polymer is mesoporous and the mesopore size is around 3 nm (Fig. 1b and 1c). The FT-IR spectra indicate that PAM is successfully synthesized (Fig. S1, ESI†). The thermogravimetric analysis shows the initial decomposition temperature of PAM is above 270 °C (Fig. S2, ESI†).

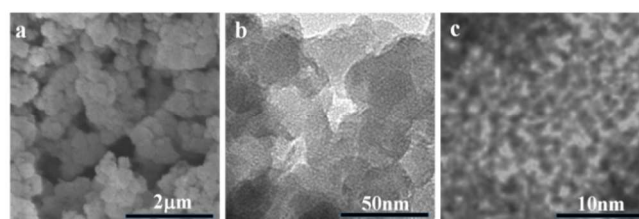


Fig. 1 SEM (a) and TEM (b, c) images of the PAM synthesized in $[C_4\text{mim}][\text{BF}_4]$.

The mesoporosity properties of the PAM were investigated by N_2 adsorption-desorption method. As shown in Fig. 2, the N_2 adsorption-desorption isotherm exhibits a mode of the type IV, which indicates that the material is mesoporous. The BET (Brunauer, Emmett, and Teller) surface area and total pore volume of the PAM synthesized in $[C_4\text{mim}][\text{BF}_4]$ are $182.2 \text{ m}^2\text{g}^{-1}$ and $0.402 \text{ cm}^3\text{g}^{-1}$, respectively. The mesopore size distribution curve, calculated from Barrett-Joyner-Halenda method, shows a pore size distribution centered at around 3.8 nm (inset of Fig. 2), which is consistent with the result derived from TEM.

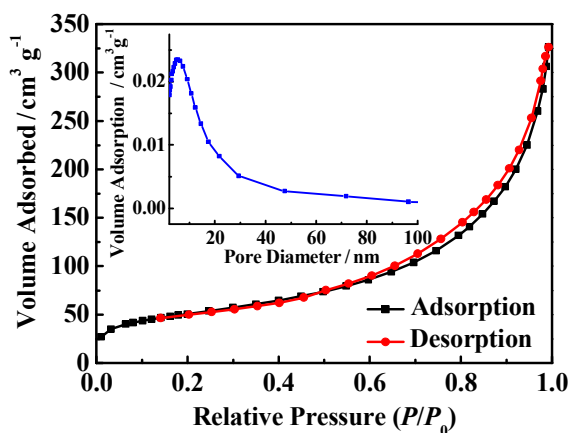


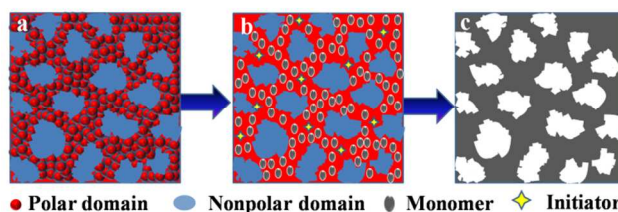
Fig. 2 N_2 adsorption-desorption isotherm and mesopore size distribution curve (the inset) of the PAM synthesized in $[C_4mim][BF_4]$.

The PAMs were synthesized in other ILs, 1-hexyl-3-methylimidazolium tetrafluoroborates ($[C_6mim][BF_4]$), 1-octyl-3-methylimidazolium tetrafluoroborates ($[C_8mim][BF_4]$), and 1-decyl-3-methylimidazolium tetrafluoroborates ($[C_{10}mim][BF_4]$), with all the experimental conditions being the same as those above. The FT-IR spectra, TGA and N_2 adsorption-desorption isotherms were also determined (Fig. S3-S5, ESI[†]). The results show that all the PAMs synthesized present mesoporous structures. The mesopore properties are summarized in Table 1. The PAM synthesized in $[C_6mim][BF_4]$ has a mesopore size of 5.4 nm, larger than that of the PAM synthesized in $[C_4mim][BF_4]$ (No. 1 and 2). The increased mesopore size may be due to the swelling of nonpolar domains with the increasing alkyl length of IL.³² There is no obvious changes for the mesopore size of the PAMs synthesized in $[C_6mim][BF_4]$, $[C_8mim][BF_4]$ and $[C_{10}mim][BF_4]$ (No. 2-4). It may result from the percolation of the non-polar domains in the midst of a continuous polar network to form a bi-continuous segregated phase at larger alkyl length of IL (C_6 , C_8 , C_{10}).³²

Table 1 The mesopore diameter (D_{meso}), BET surface area (S_{BET}) and mesopore volume (V_i) of the PAMs synthesized in different ILs.

No.	ILs	D_{meso}/nm	S_{BET}/m^2g^{-1}	V_i/cm^3g^{-1}
1	$[C_4mim][BF_4]$	3.8	182.2	0.402
2	$[C_6mim][BF_4]$	5.4	191.7	0.503
3	$[C_8mim][BF_4]$	5.7	113.0	0.314
4	$[C_{10}mim][BF_4]$	5.8	91.9	0.222

A possible mechanism for the mesoporous polymer formation in IL was proposed (Scheme 1). The nanostructure in pure IL is illustrated in Scheme 1a. The imidazolium ring and the groups of the cation as well as the anions form polar domains, which contain around 90% of the electron charges in the IL, while the alkyl chains of IL aggregate to form nonpolar domains.^{31,32} For the polymerization, the monomer acrylamide and initiator $K_2S_2O_8$ are dissolved in the polar domains where the polymerization occurs; therefore, the nonpolar domains function as templates for the mesopore formation (Scheme 1b). After reaction and the removal of IL by washing, the mesoporous polymer is formed (Scheme 1c).



Scheme 1 Schematic illustration for the formation of mesoporous polymer.

Mesoporous polymers have potential use for the dispersion of small metal nanoparticles as catalyst support.³³ Herein we utilized the as-synthesized mesoporous PAM as a support for Pd catalyst. Fig. 3a shows the TEM images of the Pd/PAM composite. The nanoparticles in size of 4-10 nm are highly dispersed in the polymer. From the high-resolution TEM (HRTEM) image shown in Fig. 3b and 3c, the interplanar distance of the nanoparticles can be clearly observed and measured to be 0.2 nm, corresponding to Pd (200). The X-ray diffraction pattern (Fig. S6, ESI[†]) shows two characteristic diffractions corresponding to (111) and (200) planes of Pd⁰ with face centered cubic (fcc) crystalline structure. The broad diffraction at the 2θ value of 20.5 corresponds to the mesoporous polymer matrix in the catalyst. The X-ray photoelectron spectroscopy (Fig. S7, ESI[†]) reveals the presence of Pd($3d_{5/2}$) and Pd($3d_{3/2}$) peaks at binding energy values of 335.3 and 340.6 eV, respectively, further proving the formation of metallic palladium. The loading of palladium on the PAM was 3 wt%, determined by ICP-AES analysis.

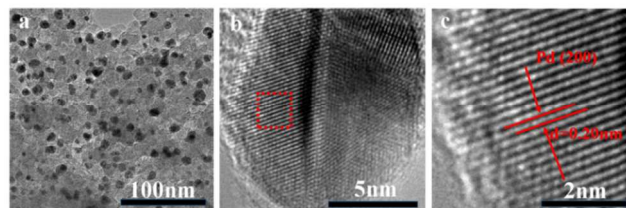


Fig. 3 TEM and HRTEM images of the Pd/PAM composite. The PAM was synthesized in $[C_4mim][BF_4]$

The hydrogenation of *p*-CNB to obtain *p*-CAN is an important reaction because *p*-CAN is an important industrial intermediate for a variety of specific and fine chemicals. However, the dehalogenation generally occurs during the catalytic reduction of *p*-CNB. To overcome this problem, the bimetallic catalyst (e.g. Pt/Pd, Ru/Pd) or/and the addition of base (e.g. NaOH, NaOAc) were needed,³⁴⁻³⁷ which unavoidably increase the economic and environmental burdens. Here the as-synthesized monometallic Pd/PAM composite was used as a catalyst for the hydrogenation of *p*-CNB to obtain *p*-CAN under a non-alkali condition. The catalytic performance of Pd/PAM composite is shown in Table 2. *p*-CNB is almost completely converted within 30 minutes at 40 °C and an H_2 pressure of 3 MPa when using a substrate/Pd molar ratio of 700 (Entry 1). The yield of *p*-CAN is 54.84% and the turnover frequency (TOF) is 672 h^{-1} . As the reaction time is increased to 1 h, the yield reaches a maximum value of 68.90% (Entry 2), and then decreases with the prolonged reaction time (Entries 3, 4). The PAMs synthesized in $[C_6mim][BF_4]$, $[C_8mim][BF_4]$ and $[C_{10}mim][BF_4]$ were also used as support for Pd nanoparticles. These Pd/PAM catalysts show highly catalytic activity and selectivity for the hydrogenation of *p*-CNB to yield *p*-CAN (Entries 5-7). For comparison, the *p*-CNB

hydrogenation was performed using a commercial Pd/C catalyst (Entry 8). The *p*-CAN yield is 44.70%, much lower than that catalyzed by the as-synthesized Pd/PAM catalyst. Moreover, for comparison with the reported data, we also performed the *p*-CNB hydrogenation using the as-synthesized Pd/PAM catalyst with an H₂ pressure of 1 atm at 65 °C. The conversion can reach 42.8% with the *p*-CAN yield of 5.32% (Entry 9); while for the Pd/poly(*N*-vinyl-2-pyrrolidone) (PVP) catalyst, the conversion at the same experimental conditions is extremely low (1.4%, Entry 10).³⁷ These results indicate that the catalytic activity of the Pd/PAM is much higher than those of the commercial Pd/C catalyst and the reported Pd/PVP catalyst for the hydrogenation of *p*-CNB to yield *p*-CAN. It can be attributed to the mesoporous polymer structure, which is favourable for the diffusion of substrates and products.³⁸

Table 2. Catalytic activity test for the hydrogenation of *p*-CNB to yield *p*-CAN.

Entry	P _{H2}	Time	conversion	Yield ^[g]	TOF ^[h]
1 ^[a]	3 MPa	30 min	100%	54.84%	672 h ⁻¹
2 ^[a]	3 MPa	60 min	100%	68.90%	490 h ⁻¹
3 ^[a]	3 MPa	90 min	100%	59.47%	280 h ⁻¹
4 ^[a]	3 MPa	120 min	100%	52.02%	189 h ⁻¹
5 ^[b]	3 MPa	60 min	100%	58.84%	480 h ⁻¹
6 ^[c]	3 MPa	60 min	100%	66.78%	510 h ⁻¹
7 ^[d]	3 MPa	60 min	100%	60.79%	504 h ⁻¹
8 ^[e]	3 MPa	60 min	100%	44.70%	191 h ⁻¹
9 ^[a]	1 atm	56 min	42.8%	5.32%	55 h ⁻¹
10 ^[f]	1 atm	56 min	1.4%	-	-

Reaction conditions: temperature: 40 °C for Entries 1-8, 65 °C for Entries 9 and 10. Substrate/Pd (mol/mol) = 700 (Entries 1-8), Substrate/Pd (mol/mol) = 1035 (Entries 9 and 10). The PAMs were synthesized in [a] C₄mimBF₄ [b] C₆mimBF₄ [c] C₈mimBF₄ [d] C₁₀mimBF₄. [e] The commercial Pd/C catalyst. [f] The Pd/PVP catalyst reported in Ref 37. [g] Yield of *p*-CAN by the hydrogenation of *p*-CNB. [h] Turnover number (TON) = mol of product (*p*-CAN) per mole of Pd, turnover frequency (TOF) = TON·h⁻¹.

Conclusions

In summary, we have reported the template-free synthesis of mesoporous polymers in ILs for the first time. The mesopore porosities of the polymer can be tuned by the alkyl chain length of the IL. This method for mesoporous polymer formation is template-free, involves no organic solvent and is more environmentally benign. The as-synthesized PAM can be used as catalyst support and the Pd/PAM catalyst shows highly catalytic activity and selectivity for the hydrogenation of *p*-CNB to yield *p*-CAN. The as-synthesized mesoporous polymers merge the properties of both mesoporous materials and polymers, and have potential applications in catalysis, gas storage and separation, controlled drug release, etc.

We thank the National Natural Science Foundation of China (21173238, 21133009, U1232203, 21021003), Chinese Academy of Sciences (KJCX2.YW.H16).

Notes and references

Beijing National Laboratory for Molecular Sciences, CAS Key Laboratory of Colloid and Interface and Thermodynamics, Institute of Chemistry, Chinese Academy of Sciences, Beijing 100190, P. R. China
Fax: +86-10-62559373; Tel: +86-10-62562821; E-mail: zhangjl@iccas.ac.cn

- † Electronic Supplementary Information (ESI) available: Materials, experimental details, and characterization. See DOI: 10.1039/b000000x/
- Z. Yang, Y. Lu and Z. Yang, *Chem. Commun.*, 2009, 2270-2277.
 - J. R. Holst and A. I. Cooper, *Adv. Mater.*, 2010, **22**, 5212-5216.
 - M. T. Gokmen and F. E. Du Prez, *Prog. Polym. Sci.*, 2012, **37**, 365-405.
 - A. Muñoz-Bonilla, M. Fernández-García and J. Rodríguez-Hernández, *Prog. Polym. Sci.*, 2014, **39**, 510-554.
 - D. Wu, F. Xu, B. Sun, R. Fu, H. He and K. Matyjaszewski, *Chem. Rev.*, 2012, **112**, 3959-4015.
 - T. W. Kim, I. I. Slowing, P. W. Chung and V. S-Y. Lin, *ACS nano*, 2010, **5**, 360-366.
 - T. Chen, B. Du and Z. Fan, *Langmuir*, 2012, **28**, 15024-15032.
 - Y. Zhang, S. Wei, F. Liu, Y. Du, S. Liu, Y. Ji, T. Yokoi, T. Tatsumi and F. S. Xiao, *Nano Today*, 2009, **4**, 135-142.
 - S. Samitsu, R. Zhang, X. Peng, M. R. Krishnan, Y. Fujii and I. Ichinose, *Nat. Commun.*, 2013, **4**, 2653.
 - N. Brun, S. R. S. Prabaharan, C. Surcin, M. Morcrette, H. Deleuze, M. Birot, O. Babet, M. F. Achard and R. Backov, *J. Phys. Chem. C*, 2012, **116**, 1408-1421.
 - Y. Liang, S. Lu, D. Wu, B. Sun, F. Xu and R. Fu, *J. Mater. Chem. A*, 2013, **1**, 3061-3067.
 - Y. Wan, Y. Shi and D. Zhao, *Chem. Mater.*, 2008, **20**, 932-945.
 - N. Pal and A. Bhaumik, *Adv. Colloid Interface Sci.*, 2013, **189-190**, 21-41.
 - J. S. Wilkes, *Green Chem.*, 2002, **4**, 73-80.
 - T. D. Ho, C. Zhang, L. W. Hantao and J. L. Anderson, *Anal. Chem.*, 2014, **86**, 262-285.
 - N. V. Plechkova and K. R. Seddon, *Chem. Soc. Rev.*, 2008, **37**, 123-150.
 - T. L. Greaves and C. J. Drummond, *Chem. Rev.*, 2008, **108**, 206-237.
 - T. Torimoto, T. Tsuda, K. Okazaki and S. Kuwabata, *Adv. Mater.*, 2010, **22**, 1196-1221.
 - H. Olivier-Bourbigou, L. Magna and D. Morvan, *Appl. Catal. A*, 2010, **373**, 1-56.
 - R. Sheldon, *Chem. Commun.*, 2001, 2399-2407.
 - V. I. Pârvulescu and C. Hardacre, *Chem. Rev.*, 2007, **107**, 2615-2665.
 - Z. Ma, J. Yu and S. Dai, *Adv. Mater.*, 2010, **22**, 261-285.
 - P. Kubisa, *Prog. Polym. Sci.*, 2004, **29**, 3-12.
 - J. Lu, F. Yan and J. Texter, *Prog. Polym. Sci.*, 2009, **34**, 431-448.
 - P. Kubisa, *Prog. Polym. Sci.*, 2009, **34**, 1333-1347.
 - R. Vijayaraghavan and D. R. MacFarlane, *Chem. Commun.*, 2004, 700-701.
 - C. Guerrero-Sanchez, T. Erdmenger, P. Šereda, D. Wouters and U. S. Schubert, *Chem. Eur. J.*, 2006, **12**, 9036-9045.
 - L. Zhu, C. Y. Huang, Y. H. Patel, J. Wu and S. V. Malhotra, *Macromol. Rapid Commun.*, 2006, **27**, 1306-1311.
 - J. S. Li, J. L. Zhang, Y. J. Zhao, B. X. Han and G. Y. Yang, *Chem. Commun.*, 2012, **48**, 994-996.
 - L. Peng, J. L. Zhang, J. S. Li, B. X. Han, Z. M. Xue and G. Y. Yang, *Angew. Chem. Int. Ed.*, 2013, **125**, 1836-1839.
 - J. N. A. Canongia Lopes and A. A. H. Pádua, *J. Phys. Chem. B*, 2006, **110**, 3330-3335.
 - K. Shimizu, M. F. Costa Gomes, A. A. H. Pádua, L. P. N. Rebelo and J. N. C. Lopes, *J. Mol. Struct.*, 2010, **946**, 70-76.
 - F. Cárdenas-Lizana, C. Berguerand, I. Yuranov and L. Kiwi-Minsker, *J. Catal.*, 2013, **301**, 103-111.
 - Q. Xu, X. M. Liu, J. R. Chen, R. X. Li and X. J. Li, *J. Mol. Catal. A*, 2006, **260**, 299-305.
 - F. Cárdenas-Lizana, S. Gómez-Quero, A. Hugon, L. Delannoy, C. Loid and M. A. Keane, *J. Catal.*, 2009, **262**, 235-243.
 - F. Cárdenas-Lizana, Y. Hao, M. Crespo-Quesada, I. Yuranov, X. Wang, M. A. Keane and L. Kiwi-Minsker, *ACS Catal.*, 2013, **3**, 1386-1396.
 - Z. Yu, S. Liao, Y. Xu, B. Yang and D. Yu, *J. Mol. Catal. A*, 1997, **120**, 247-255.
 - W. Xuan, C. Zhu, Y. Liu and Y. Cui, *Chem. Soc. Rev.*, 2012, **41**, 1677-1695.